Evidence of power law decay of superexchange coupling in a disordered two-dimensional π-electron system

K. Bagani,[1] M. K. Ray,[1] M. Sardar,[2] and S. Banerjee[1,*]

[1]*Surface Physics and Material Science Division, Saha Institute of Nuclear Physics, 1/AF Bidhannagar, Kolkata-700064, India*
[2]*Materials Science Group, Indira Gandhi Centre for Atomic Research, Kalpakkam-603102, India*

We report the specific heat of graphite, highly oriented pyrolytic graphite (HOPG), graphene oxide (GO), and reduced graphene oxide (RGO) from 300 K to 50 mK. Graphite and HOPG exhibits transition from three dimensions ($C_v \propto T^3$) to two dimensions ($C_v \propto T^2$) as the temperature increases above 4 K and approaching linearity in temperature for both around room temperature is observed. We observe a Schottky-like peak in specific heat of graphene oxide and reduced graphene oxide near 0.1 K, whose intensity and peak position varies with external magnetic field. We find that the random Heisenberg superexchange interaction between the Anderson (disorder) localized π electrons of GO/RGO is responsible for the specific-heat peak. The exchange interaction strength between the localized spins falls off with distance as a weak power law ($\propto \frac{1}{r^{2.5}}$), rather than the usual exponential fall in insulating magnets.

Two dimensional (2D) graphene exhibits unique electronic properties [1,2] and presence of localized defects and extended defects like edges gives rise to unconventional magnetic properties [3,4]. But the least investigated among all is the specific heat of 2D graphene systems. Low-temperature specific heat provides key insights about many physical properties such as structural, magnetic, and superconducting phase transition because it contains the information about the electronic density of states at the Fermi level and low-energy (collective) excited states. Theoretical calculation by Benedict *et al.* [5] shows that in graphene the lattice contribution to the specific heat is almost 1000 times larger than the electronic contribution at all temperatures. Hence, it is expected that the phonon specific heat will dominate down to $T \to 0$ K. Phonon specific heat at low temperature is $C_v \sim T^{d/n}$, where d is the dimension and n is the exponent in the phonon energy (ω) momentum (k) relation, $\omega(k) \sim k^n$. Carbon nanotube (1D), graphene (2D), highly oriented pyrolytic graphite (HOPG) (weakly coupled 2D planes), and graphite (3D) are ideal systems to study the dimensional dependence of specific heat as their basic structural element is the same. 2D graphene has three acoustic-phonon modes. Two in-plane modes [longitudinal (LA) and transverse (TA)] which have a linear energy-momentum dispersion giving $C_v \propto T^2$ and a third mode called the flexural mode [in which the atoms vibrate out of plane (ZA)] with a dispersion relation $\omega(k) = k^2$ giving $C_v \propto T$ [6]. Compared to the LA and TA modes where the atoms, connected by strong σ bonds, vibrate in the plane, the excitation of the ZA mode is of lower energy. Thus the phonon specific heat for 2D graphene should be composed of a linear (ZA phonon) plus a quadratic (LA/TA phonons) component, with the linear term dominating at all temperatures [6,7]. Low-temperature specific heat of a collection of 1D carbon nanotubes (CNTs) has been well studied [8,9] but, there are no experimental studies on graphene so far.

Lattice specific heat of natural 3D graphite is expected to be T^3 ($d = 3, n = 1$) at very low temperature. DeSorbo *et al.* [10] have seen a T^3 behavior below 3 K and a T^2 dependence in the temperature range 13–54 K indicating that at higher temperatures the system behaves like a 2D system. Komatsu [11] also finds that above 20 K the specific heat of graphite deviates from T^3 to T^2 dependence and there is a linear T dependence of electronic contribution at very low temperatures ($T < 1$ K) indicating finite electron density of states at the Fermi level. The specific heat of a system depends not only on the dimension but also on the defects in the structure. Viana *et al.* [12] have reported a $T^{-0.57}$ dependence below 0.5 K in exfoliated graphite arising due to the interaction between the localized states. A similar type of behavior was also observed in phosphorus doped silicon [13] and was well explained by Bhatt and Lee [14]. If the electrons are in the localized regime, the electrons are left with only the spin degrees of freedom and the electronic specific heat comes from thermal population of all states with different spin configurations.

In this paper, we have reported the specific heat of graphite, highly oriented pyrolytic graphite (HOPG), graphene oxide (GO), and reduced graphene oxide (RGO) from 300 K down to 50 mK. Graphite and HOPG were commercially procured whereas GO and RGO were synthesized from graphite powder using modified Hummer's method [15]. Synthesis and characterization of GO and RGO are reported elsewhere [16]. Specific heat of the samples from 300 to 2 K was measured using a physical property measurement system (PPMS, Quantum Design) and from 4 K to 50 mK was measured using a PPMS-DR (dilution refrigerator) system. In between 2 and 4 K the two sets of measured data join smoothly. We observed no linear T electronic specific heat in GO and RGO; instead the specific heat below 0.5 K shows a Schottky-like peak near 100 mK and a slow falling tail above the peak temperature. Under external magnetic field, the peak shifts towards higher temperatures and the peak value of specific heat increases. We have modelled the electronic system in GO and RGO as composed of some paramagnetic

---

*sangam.banerjee@saha.ac.in
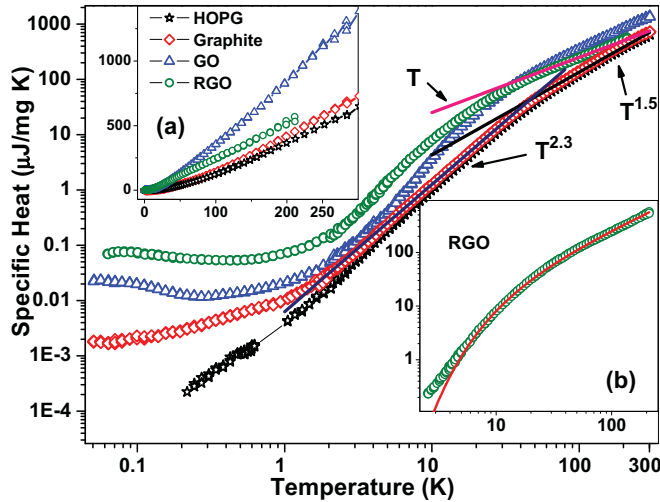
FIG. 1. (Color online) Specific-heat data of graphite, HOPG, GO, and RGO in log-log scale and the same in linear scale in inset (a). Inset (b): Fitting of RGO specific-heat data.

noninteracting π electron with spin-$\frac{1}{2}$ moments, coexisting with interacting π electrons. The interaction Hamiltonian is a random antiferromagnetic (superexchange) Heisenberg model for dilute spin-$\frac{1}{2}$ moments [13,14,17,18]. This peak is absent in graphite and HOPG but we find that graphite has an excess $T^{-0.14}$ contribution below 1 K and we attribute this to the localized electrons at the defect centers which gives rise to the specific-heat peak in GO and RGO as we shall see below. We have also analyzed the specific heat beyond 1 K in graphite, HOPG, GO, and RGO, entirely in terms of lattice phonon, and find that the systematic changes in lattice specific heat in these four systems share some universal features which we shall point out here. We have measured resistance vs temperature of RGO from 300 to 2 K using the four-probe method to understand the nature of the disorder.

Figure 1 shows the specific heat of all the samples. Specific heat of both HOPG and graphite varies as $T^{1.5}$ in 80–300-K range. This switches over smoothly to $T^{2.3}$ behavior in the 5–50-K range. This type of behavior has been reported earlier [10,11,19,20]. In Fig. 2(a) a C_V/T vs $T^{1.65}$ plot of HOPG shows linearity in the range 240 mK–4 K indicating that the specific heat of HOPG follows the $aT + bT^{2.65}$ from 240 mK to 4 K, with coefficients $a = 1.1 \times 10^{-3}$ μJ/mg/K and $b = 2.5 \times 10^{-3}$ μJ/mg/K$^{2.65}$. $T^{2.65}$ dependence indicates that both $T^2(d = 2, n = 1)$ and $T^3(d = 3, n = 1)$ terms are present in the phonon specific heat due to weak coupling between the layers. C_V/T vs T^2 plot of graphite in Fig. 2(b) shows a straight line in the temperature range 500 mK–4 K, hence the specific heat of graphite fits to the $aT + bT^3$ form in this temperature range, with $a = 9.7 \times 10^{-3} \mu$J/mg/K, and $b = 1.6 \times 10^{-3} \mu$J/mg/K^3. Coefficient a is proportional to the density of states at the Fermi level. Graphite has more density of states than HOPG. In the temperature range 5–300 K, specific heat does not have any T^3 term, showing that the z-axis dispersive 3D phonon contribution saturates beyond 5 K. So at higher temperature, the specific heat of 3D graphite is basically similar to HOPG. Hoeven *et al.* [20] finds a T^3 dependence below 2 K, with a gradual transition from T^3 to
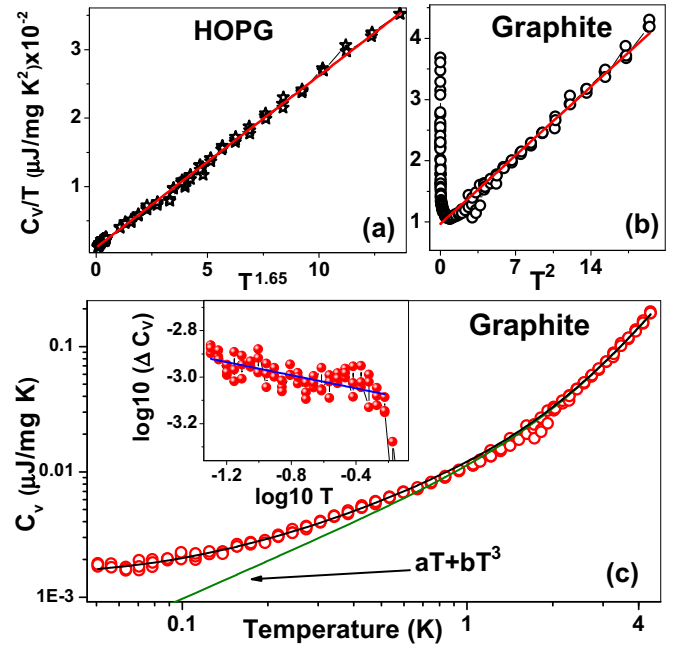
FIG. 2. (Color online) (a) C_V/T vs $T^{1.65}$ plot of HOPG. (b) C_V/T vs T^2 plot of graphite. (c) Specific-heat data of graphite from 50 mK to 4 K fitted with the form $C_v = aT + bT^3 + pT^{-0.14}$. Inset: $\log_{10}(\Delta C_V)$ vs $\log_{10} T$ plot.

T^2 dependence from 2 to 20 K and pure T^2 dependence above 20 K. The linear T-dependent specific heat due to the flexural phonon is suppressed at low temperatures in both graphite and HOPG, due to nonzero gap in flexural modes because of interlayer coupling between the planes. This mode dominates near room temperature. Hence the specific heat of graphite and HOPG smoothly change over from T^3 below 4 K to $T^{2.3}$ behavior in the 5–50-K range and $T^{1.5}$ in the 80–300-K range.

The specific heat of graphite is different from HOPG in a fundamental way only below 0.5 K, where C_V/T keeps rising with decreasing temperature. We find that the specific-heat data of graphite can be fitted with $C_v = aT + bT^3 + pT^{-0.14}$ down to 50 mK [Fig. 2(c)]. An extra $pT^{-0.14}$ contribution is obtained from $\log_{10}(\Delta C_V)$ vs $\log_{10} T$ plot [Fig. 2(c) inset] where ΔC_V is the excess specific heat over the T and T^3 term. This anomalous contribution comes from the magnetic interaction of randomly distributed localized electronic states at the defect sites [12]. Structurally HOPG has lesser defects than graphite powder and hence does not have any such anomalous specific heat.

In GO and RGO the specific heat is almost linear at $T > 50$ K. Thermal energy is stored in many local vibrations of the adatoms like O and OH. Since GO has more O and OH groups than RGO, the specific heat is larger in GO than RGO at $T > 50$ K. Near 50 K, the specific heat of GO and RGO are almost the same, indicating that these local modes are frozen below 50 K. Below 50 K the specific heat decreases very fast with a sigmoid-type bend (in log scale). There is a crossing of curves at 30 K, below which specific heat of GO is surprisingly less than RGO. Even though the thermal vibrations of O and OH groups are now frozen, their presence affects the flexural mode dispersion relations and density of states. Specifically the

random attachment of O and OH on the carbon network stiffens the flexural mode and suppresses this mode leading to lowering of specific heat. One expects a redistribution of the density of state of flexural phonons, i.e., a transfer of density of states from low energy to higher energies (resulting in the formation of a pseudogap). We can phenomenologically model this by introducing a gap in the flexural phonon in RGO/GO. Above 10 K, the specific-heat data of RGO/GO can be fitted with the form $C_v = cTe^{-\frac{\Delta}{T}}$ [Fig. 1(b)] with $\Delta = 12.5$ and 45 K for RGO and GO respectively. The freezing of the linear specific heat of flexural modes at $T < \Delta$ is responsible for the sigmoid-type bends. The larger gap in GO compared to RGO is responsible for the crossing of the curves and lesser specific heat in GO compared to RGO below the crossing temperature. This means, at $T < \Delta$, specific heat due to the ZA mode is small. Here specific heat in GO and RGO should be dominated by the LA and TA modes, i.e., $C_v \propto T^2$. In the temperature range 2–10 K, the specific-heat data of GO/RGO fits with $T^{2.5}$, showing the presence of a T^3 term along with a T^2 contribution. The T^3 term comes presumably because of the presence of a small amount of few-layered GO and RGO in the materials. Multilayered graphene sheets should give a T^3 contribution due to 3D phonon modes, like in HOPG and graphite. Specific heat of GO and RGO below 1 K is purely electronic in origin and is fundamentally different from HOPG and graphite.

To understand better the electronic states in GO/RGO we have measured the temperature dependence of resistivity in RGO which is shown in Fig. 3. Resistivity can be explained by the variable range hopping (VRH) mechanism, i.e., $R = R_0 e^{(T_0/T)^p}$ where, for the Mott-VRH [21] in d dimension $p = \frac{1}{1+d}$ and for Efros-Shklovskii VRH (ES-VRH) [22] $p = 1/2$ in all dimensions when the Coulomb interaction between hopping sites are considered. From the plot of reduced activation energy $w(T) = -\frac{\delta \ln R}{\delta \ln T}$ [23] vs temperature (inset of Fig. 3), we find $p = 1/3$ in the temperature range 250–50 K and for $T < 50$ K, $p = 1/2$. It is clear that there is a crossover from Mott-VRH to ES-VRH at 50 K. Since the electrons are strongly localized at low temperatures in GO/RGO, the

specific heat at the lowest temperatures should come from the spin degrees of freedom of the localized electrons. Both GO and RGO have a peak in specific heat even in the absence of external magnetic field. Under external magnetic field H, the specific heat for a two-level system caused by Zeeman splitting ($\Delta\epsilon = 2\mu_B H$) of a localized electron is $C_v^{\text{para}}(T) = (\frac{\Delta\epsilon}{k_B T})^2 \frac{e^{-\Delta\epsilon/k_B T}}{(1+e^{-\Delta\epsilon/k_B T})^2}$. This expression has a peak at $T_{\text{peak}} = 0.417\Delta\epsilon = 0.828\mu_B H$ and also shows a peak shift to higher temperature with external magnetic field but the specific heat at the peak temperature does not change with magnetic field. For $H = 1000$ Oe, the shift in peak temperature should be 0.062 K. For RGO and GO this peak shift is 0.048 and 0.065 K, which indicates that the Schottky type specific-heat peak is due to $s = \frac{1}{2}$ localized paramagnetic moments of the π electrons in GO/RGO.

The actual magnetic field felt by a localized electron is the external field plus the internal magnetic field due to nearby moments, i.e., $H = H_{\text{ext}} + H_{\text{int}}$. From the peak temperature at $H_{\text{ext}} = 0$ Oe we get $H_{\text{int}} = 400$ Oe. C-C distance in graphene is $a_0 = 1.42 \times 10^{-8}$ cm. The magnetic dipolar field felt by an electron due to another electron at a distance $2a_0$ is $H_{\text{eff}} = \frac{\mu_B}{(2a_0)^3} = 405$ Oe. To see if the internal field is really due to an uncompensated stray magnetic dipolar field from near-neighbor $s = \frac{1}{2}$ paramagnetic π electron moments, we need to know the average separation between paramagnetic moments in GO/RGO. We use the low-field ($H = 100$ Oe) magnetic susceptibility of GO and RGO (same materials) which we have reported in Ref. [16]. Magnetic susceptibility of GO/RGO are Curie-like with Curie constants, $C = 8.05 \times 10^{-3}$ emu/g/Oe K for RGO, and $C = 1.8 \times 10^{-2}$ emu/g/Oe K for GO. The Curie constant from N moments (per gram) of $S = 1/2$ is $C = N\frac{4\mu_B^2}{3k_B}S(S+1)$. We find $N = 1.11 \times 10^{22}$ and 2.46×10^{22} in RGO and GO respectively. The number of carbon atoms/g is 5×10^{22}. This means only a fraction of 0.22 and 0.48 of the carbon sites have moments, which gives paramagnetic moment in RGO and GO respectively. So the average separation between the paramagnetic moments are $2.13a_0$ and $1.44a_0$ in RGO and GO and hence we may conclude that the internal field is magnetic dipolar in origin. Observation of a lesser number of paramagnetic $s = 1/2$ moments in RGO compared to GO suggests the presence of antiferromagnetic interaction between these localized π electrons. Nearest-neighbor π electrons with antiferromagnetic interaction favors singlet formation and singlets do not contribute to the low-field magnetic susceptibility. Since RGO has more π electrons than GO, it also has a larger number of nearest-neighbor singlets than GO. This is the reason for the observation of low magnetization in RGO compared to GO.

The experimentally measured specific heat has two additional features that cannot be explained by the paramagnetic moments, i.e., (1) the value of specific heat at the peak temperature increases with magnetic field and (2) the specific heat drops slower than $\frac{1}{T^2}$ for $T > T_{\text{peak}}$ which indicates that the additional contribution to the specific heat arises from the interacting spins. Natural interaction between the electrons is of superexchange type and so we can model the interacting electrons by an effective Hamiltonian, $H = \sum_{i,j} J_{ij} S_i S_j$ where the spins are at random sites and the number of spins is less than the number of lattice sites in GO/RGO. We shall
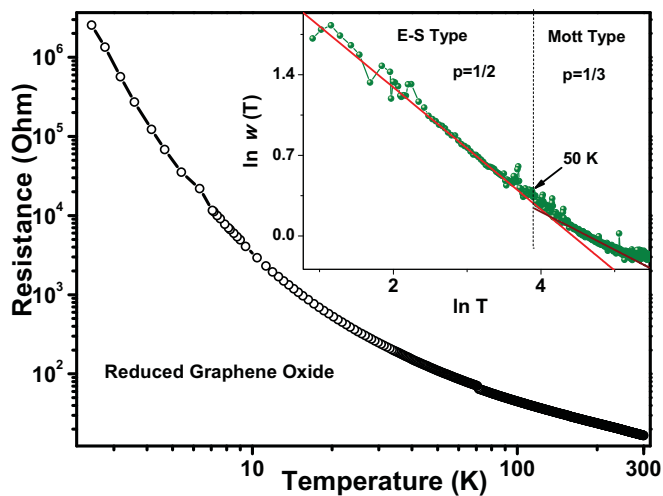
FIG. 3. (Color online) Resistance vs temperature plot of RGO in log-log is scale showing nonlinear behavior. Inset: $\ln w(T)$ vs $\ln T$ plot of RGO.

assume a functional form for J_{ij} as a function of distance between the spins $|R_i - R_j|$. For spin $S = \frac{1}{2}$, there is a strong tendency towards formation of spin singlets between pairs of electrons. For N spin-1/2 electrons, there exists a large number of ways to pair them up into $\frac{N}{2}$ singlet pairs. At any finite temperature T all pairs with exchange energy $J > T$ are frozen into singlets and the specific heat comes from the rest of the pairs with $J < T$.

In the absence of magnetic field the ground state of two electrons with exchange coupling J is $\frac{1}{\sqrt{2}}[\uparrow\downarrow - \downarrow\uparrow]$ with

energy $-\frac{3}{4}J$ and three states $[\uparrow\uparrow]$, $[\downarrow\downarrow]$, and $\frac{1}{\sqrt{2}}[\uparrow\downarrow + \downarrow\uparrow]$ are degenerate with energy $+\frac{1}{4}J$, so the energy separation is J. By rescaling, the partition function is $Z = 1 + 3e^{-J/T}$ and the specific heat of two electrons is $C_v^{\mathrm{pair}}(J,T) = 3 \times (\frac{J}{T})^2 \frac{e^{-J/T}}{(1+3e^{-J/T})^2}$. In the presence of field ($H \neq 0$) the energy of the two states, $\frac{1}{\sqrt{2}}[\uparrow\downarrow - \downarrow\uparrow]$ and $\frac{1}{\sqrt{2}}[\uparrow\downarrow + \downarrow\uparrow]$ do not change. The energy of $[\uparrow\uparrow]$ and $[\downarrow\downarrow]$ becomes $J - 2\mu_B H$ and $J + 2\mu_B H$ respectively and in this case the specific heat of two electrons is

$$C_v^{\mathrm{pair}}(J,T,H) = \frac{e^{-J/T}\left[J^2 + 4a^2 e^{-J/T} + 2(J^2+a^2)\cosh\frac{a}{T} + 2a^2 e^{-J/T}\cosh\frac{a}{T} - 4Ja\sinh\frac{a}{T}\right]}{T^2\left[1 + e^{-J/T} + 2e^{-J/T}\cosh\frac{a}{T}\right]^2},$$

where $a = 2\mu_B H$. Similarly there will be singlet pairs of all bond lengths r with exchange coupling $J(r)$. The number of bonds whose length is between r and $r + dr$ is $N(r)dr = \frac{N}{A} \times 2\pi r dr$ where N is the total number of interacting spins and A is the total area. So the total specific heat is $C_{v,N}^{\mathrm{pair}}(T,H) = \frac{2\pi N}{A} \times \int_{a_0}^{\infty} r dr C_v^{\mathrm{pair}}(J(r),T,H)$. With this formula, we find good fittings with the experimental data by considering power law decay of $J(r)$ rather than the exponential decay. If we assume the superexchange coupling $J(r) = J_0(\frac{a_0}{r})^n$ where a_0 is the localization length then the specific heat is $C_{v,N}^{\mathrm{pair}} = N\frac{2\pi a_0^2}{nA}\int_{X_{\min}}^{X_0}\frac{dX}{X} \times (\frac{X}{X_0})^{2/n} \times C_v(J(r),T,H)$, where $X = \frac{J}{T}$ and $X_0 = \frac{J_0}{T}$. We must emphasize that the lower limit on J or X cannot be set to zero in this formula. There has to be a lower cutoff which will bring down the rising specific heat to zero in the $T \to 0$ limit. Strictly the $J = 0$ limit corresponds to paramagnetic moments whose specific heat we have already discussed. Hence, the total specific heat of the system is $C_v^{\mathrm{Total}}(T,H) = K_1 C_v^{\mathrm{para}}(T,H) + K_2 C_{v,N}^{\mathrm{pair}}(T,H)$. We find the best fit with $n = 2.5$ and $J_0 = 5$ K as shown in Figs. 4(c) and 4(d) where ΔC_v is the remaining specific heat after substraction of the phonon contribution ($cT^{2.6}$ for RGO and $cT^{2.5}$ for GO) at low temperature. The extracted values of K_1 and K_2 are independent of magnetic field and are 0.123 and 0.154 μJ/mg/K in RGO and 0.05 and 0.04 μJ/mg/K in GO. $\frac{K_1}{2K_2}$ is equal to the ratio of the number of paramagnetic and interacting moments. This ratio is 1.25 in GO and 0.8 in RGO which is expected because RGO has lower magnetization than GO. Variable range hopping (VRH) conductivity presupposes exponentially localized wave functions and since the superexchange coupling energy is proportional to the square of the wave function overlap between two electrons, the superexchange coupling should fall exponentially with distance. However, we find that a power law falloff with distance of exchange coupling gives a more satisfying fit of specific heat of both GO/RGO at $H = 0$ and 1000 Oe than the exponential fall. Recent theoretical work on disordered graphene [24] within a T-matrix approximation predicts power law fall of charge density of the localized state (as $\propto \frac{1}{r^{0.5}}$) coming entirely due to linear dispersion of electrons. For such power law localized states, the superexchange

coupling should be $J(r) \propto \frac{1}{r}$. Our analysis of specific-heat data suggests that $J(r) \propto \frac{1}{r^{2.5}}$, i.e., a much faster falloff with distance. This difference is most likely due to neglection of Coulomb interaction between the electrons in Ref. [24].

In conclusion, we find that the π electrons in GO and RGO are in Mott-Anderson localized states due to disorder scattering. Localized electrons have random antiferromagnetic Heisenberg exchange interaction between them. There is strong singlet pairing correlation in the system with existence of singlet bonds of all length scales. The superexchange coupling between the moments in this system is found to fall as a power law with distance between them. This is radically different from all known magnetic insulators where superexchange coupling falls exponentially with separation.
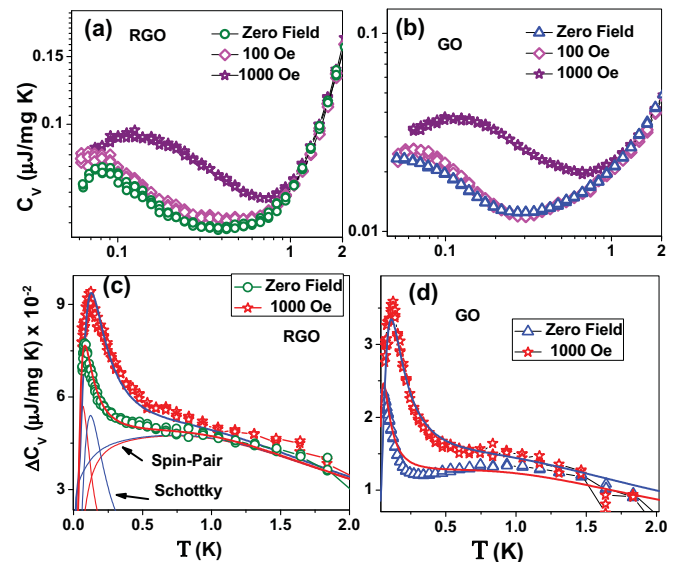
FIG. 4. (Color online) (a), (b) Low-temperature specific-heat data in log-log scale of RGO and GO respectively in presence of 0-, 100-, and 1000-Oe field. (c), (d) Fittings of low-temperature specific-heat peak of RGO and GO respectively with Schottky peak and spin pair model after subtraction of phonon contribution.

[1] H. C. Neto, F. Guinea, N. M. R. Peres, K. S. Novoselov, and A. K. Geim, Rev. Mod. Phys. **81**, 109 (2009).

[2] A. K. Geim and K. S. Novoselov, Nat. Mater. **6**, 183 (2007).

[3] V. M. Pereira, F. Guinea, J. M. B. Lopes dos Santos, N. M. R. Peres, and A. H. Castro Neto, Phys. Rev. Lett. **96**, 036801 (2006).

[4] K. Bagani, M. K. Ray, B. Satpati, N. R. Ray, M. Sardar, and S. Banerjee, J. Phys. Chem. C **118**, 13254 (2014).

[5] L. X. Benedict, S. G. Louie, and M. L. Cohen, Solid State Commun. **100**, 177 (1996).

[6] J. Hone, Topics Appl. Phys. **80**, 273 (2001).

[7] A. Mizel, L. X. Benedict, M. L. Cohen, S. G. Louie, A. Zettl, N. K. Budraa, and W. P. Beyermann, Phys. Rev. B **60**, 3264 (1999).

[8] J. Hone, B. Batlogg, Z. Benes, A. T. Johnson, and J. E. Fischer, Science **289**, 1730 (2000).

[9] V. N. Popov, Phys. Rev. B **66**, 153408 (2002).

[10] W. DeSorbo and G. E. Nichols, J. Phys. Chem. Solids **6**, 352 (1958).

[11] K. Komatsu, J. Phys. Soc. Jpn. **10**, 346 (1955).

[12] R. Viana, H. Godfrin, E. Lerner, and R. Rapp, Phys. Rev. B **50**, 4875 (1994).

[13] M. Straub, K. Kirch, and H. v. LShneysen, Z. Phys. B **95**, 31 (1994).

[14] R. N. Bhatt and P. A. Lee, Phys. Rev. Lett. **48**, 344 (1982).

[15] W. Hummers and R. Offeman, J. Am. Chem. Soc. **80**, 1339 (1958).

[16] K. Bagani, A. Bhattacharya, J. Kaur, A. Rai Chowdhury, B. Ghosh, M. Sardar, and S. Banerjee, J. Appl. Phys. **115**, 023902 (2014).

[17] N. Kobayashi, S. Ikehata, S. Kobayashi, and W. Sasaki, Solid State Commun. **32**, 1147 (1979).

[18] M. Lakner and H. v. Lohneysen, Phys. Rev. Lett. **63**, 648 (1989).

[19] U. Bergenlld, R. W. Hill, F. J. Webb, and J. Wilks, Philos. Mag. Ser. **45**, 851 (1954).

[20] B. J. C. van der Hoeven and P. H. Keesom, Phys. Rev. **130**, 1318 (1963).

[21] N. F. Mott and E. A. Davis, *Electronic Processes in Non-Crystalline Materials*, 2nd ed. (Clarendon, Oxford, 1979).

[22] A. L. Efros and B. I. Shklovskii, J. Phys. C **8**, L49 (1975).

[23] A. G. Zabrodskii, Philos. Mag. B **81**, 1131 (2001).

[24] S.-Z. Liang and J. O. Sofo, Phys. Rev. Lett. **109**, 256601 (2012).